Proceedings of the 2006 IEEE International Conference on Robotics and Automation
Orlando, Florida - May 2006

Integrated Design of IPMC Actuator/Sensor

Masaki Yamakita*†, Akio Sera*, Norihiro Kamamichi*, Kinji Asaka‡ and Zhi-Wei Luo†
* Department of Mechanical and Control Engineering, Tokyo Institute of Technology
2-12-1 Oh-okayama, Meguro-ku, Tokyo, JAPAN
† Bio-Mimetic Control Research Center, The Inst. of Physical and Chemical Research (RIKEN)
2271-130 Anagahora, Shimoshidami, Moriyama-ku, Nagoya, JAPAN
‡ Research Inst. for Cell Eng., National Inst. of Advanced Industrial Science and Technology (AIST)
1-8-31 Midorigaoka, Ikeda, Osaka, JAPAN
Email: {yamakita,sera,nkama}@ac.ctrl.titech.ac.jp, asaka-kinji@aist.go.jp, luo@bmc.riken.jp

***Abstract*— We are studying about robotic application of Ionic Polymer-Metal Composite (IPMC). The characteristics of IPMC highly depend on the type of counter-ions, and it is considered that the performance of the actuators can be improved by combining the actuators with several types of counter-ions and applying an integrated control. IPMC has also a sensor function, as the IPMC film generates electromotive force when it is deformed. It has possibility to be integrated into IPMC actuator with soft actuation. In this paper, we consider an integrated design of IPMC actuator/sensor, and investigate a control of the combined IPMC actuators using H_∞ control and the construction of IPMC sensor system.**

I. INTRODUCTION

A. Ionic Polymer-Metal Composite (IPMC)

Ionic Polymer-Metal Composite (IPMC) [1], which is known as also Ionic Conducting Polymer gel Film (ICPF), is one of the most promising Electro-Active Polymer (EAP) actuators [2] for applications. It is produced by plating gold or platinum chemically on a perfluorosulfonic acid membrane which is known as an ion-exchange membrane. When voltage is applied between the both metal layers, the IPMC film bends rapidly (Fig. 1). This phenomenon was discovered by Oguro et al. in 1992 [1]. The characteristics of IPMC are as follows:

- Driven by low voltage. (1∼2 [V])
- Fast response. (> 100 [Hz])
  (The maximum speed depends on the thickness, counter ion, etc.)
- Durable and stable chemically.
  (It is possible to bend over 1×10^6 times)
- Flexible.
- Movable in water or wet condition.
- Possibility of miniaturization and weight saving.
- Silent.

By exploiting these characteristics, IPMC actuators have been applied to robotic applications such as a fish-type robot [3]–[6], a snake-like robot [7], a wiper for nanorover [8], micromanipurator [9], a distributed actuation system [9], and so on.

IPMC has good property of response and durability, furthermore, it also has noteworthy properties of doping capability and sensor function. In this paper, we focus on these properties to enhance the functions of IPMC actuator/sensor. Based on the properties, we consider an integrated design of IPMC actuator/sensor.

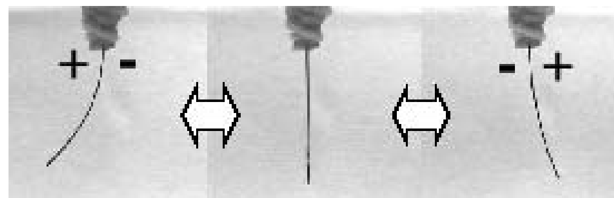

Fig. 1. Bending behavior of IPMC actuator.

B. Doping Capability

It is known that IPMC changes the bending characteristics with respect to the doped counter ions [10]. In applying to mechanical systems such as a robot, there are possibilities to change the properties of the dynamics according to an environment or a purpose adequately. We have called this property "doping effect", and verified the effect on some robotic systems.

Figure 2 shows the responses of IPMC actuator, for the same input voltage of 2.5 V, which are doped with sodium (Na^+), cesium (Cs^+) and tetraethylammonium (TEA^+) as the counter ion, respectively. From this figure, it is observed that a raising time of the actuator with Na^+ is shorter than one with Cs^+ and a raising time of one with TEA^+ is largest. On the other hand, tendency to decay of the displacement is large for the actuator with Na^+ or Cs^+ but it is very small for one with TEA^+. The counter ions are easily doped by just putting IPMC films in a solution containing the target counter ions, and higher condensed counter ions are doped into IPMC films. Also, the change of the doped ions is reversible.

It is considered that a good actuator can be made by combining the several IPMC actuators that are doped with different counter-ions and have different characteristics. In Sec. 2, we will couple the IPMC actuator doped with TEA^+ which has high gain in low frequency and that doped with Na^+ which has high gain in high frequency, and we consider a design of the appropriate feed-forward controller based on H_∞ control theory in order to realize an efficient actuating system.

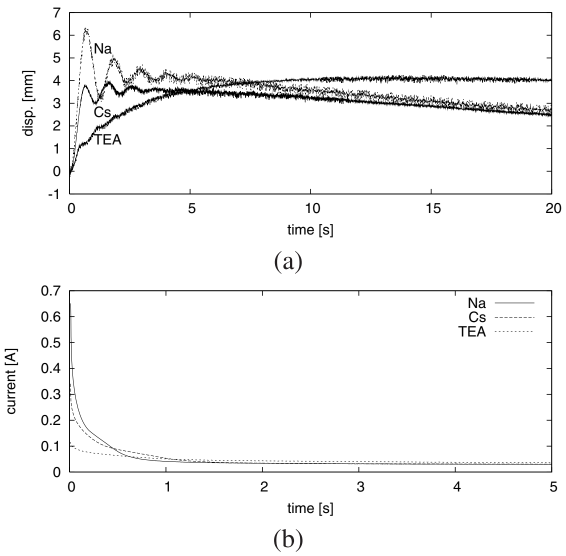

Fig. 2. Response with various counter-ions. (a) Displacement. (b) Current.

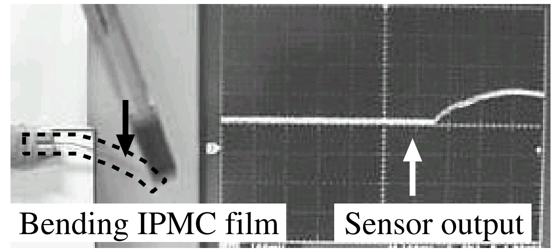

Fig. 3. IPMC sensor.

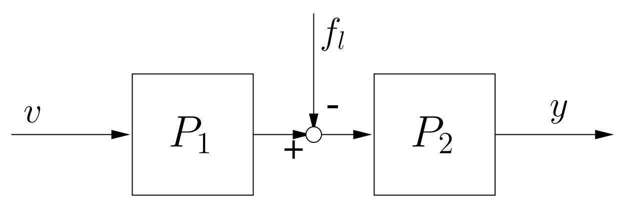

Fig. 4. LTI model of IPMC actuator.

C. IPMC Sensor

It is known that IPMC also has a sensor function, as the IPMC films generate electromotive force when it is deformed as in Fig. 3.

M. Shahinpoor et al. [11], [12] reported that the output of IPMC sensor had quasi-static relationship to the displacement, and that the IPMC was usable as a motion sensor or a pressure sensor. Konyo et al. [13] reported that the velocity of deformation was in proportion to a sensor output voltage, and the modeling and simulation of the sensor function were performed. Furthermore, the IPMC films had been already sold as a sensing device.

In order to realize the control and soft actuation of IPMC actuators, a 'soft' and 'light' sensing device is needed. Then the most effective devices is IPMC itself. IPMC has important advantage for the utilization as a sensing device:

- It is highly sensitive, and outputs voltage of mV order.
- It is usable in a wide range of deformation.
- It is flexible, and can be integrated into soft actuator system.

Some researches about qualitative property and application of the IPMC sensor were reported, however, a sensor system which measures an accurate displacement or a deformation was not constructed. In this paper, we construct an IPMC sensor system which outputs a displacement. In Sec. III, identification of sensor dynamics and construction of sensor system are explained, and feedback experiments of IPMC actuator/sensor are demonstrated.

II. Integrated Design of Combined IPMC Actuators with Various Counter-Ions

As shown in Fig. 2, the characteristics of IPMC actuator highly depend on the type of the counter-ions. The IPMC actuator doped with TEA^+ has high gain in the low frequency, on the other hand, that with Na^+ has a better property in the high frequency. It is considered that the characteristics of actuators are adjustable for purposes by selecting an appropriate counter ion or by mixing several ions in appropriate proportion.

Furthermore, it is considered that the performance of the actuators can be improved by combining the actuators with several type of counter-ions and applying an integrated control method. In order to realize an efficient activation of IPMC actuator in a wide band, we consider an integrated control of IPMC actuators with various counter-ions. In this paper, we design a feed-forward controller for the coupled IPMC actuators based on the H_∞ control theory, and confirm the efficiency of the control method.

A. Model of IPMC Actuator

As the model of the IPMC actuator, various models were considered, e.g. a black box model [9], [14] or a detailed model in consideration of the physical and electrical phenomenon [15], [16]. In this study, we consider a gray box model, and identify the dynamics of the IPMC actuator from input-output data as a linear time invariant (LTI) system. It is advantageous to use simple model which is represented by LTI system for applying the linear control theory. It was also confirmed that the model is appropriate enough and available for the control of the actuator by a feedback experiment.

Figure 4 shows the LTI model of IPMC actuator. P_1 is the transfer function from input voltage to force, P_2 is the transfer function from internal force to angle, f_l is a external force. Figure 5 shows the results of feedback control based on the identified LTI model, and position control using LQ servo controller were conducted. In this figure, the simulation result and the experimental result are plotted. From this result, the LTI model is considered to be efficient to express the characteristic of IPMC actuator.

Then, we introduce a model of coupled IPMC actuators

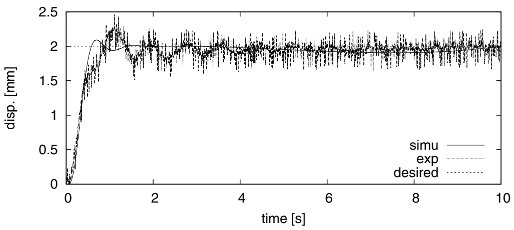

Fig. 5. Simulation and experiment of feedback control.

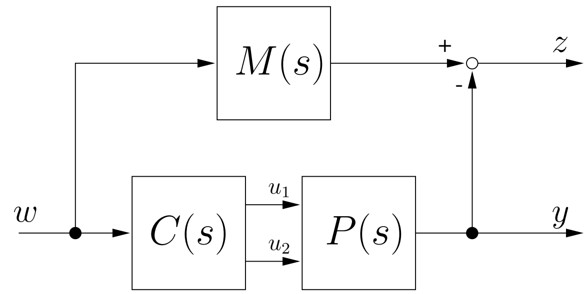

Fig. 6. Block diagram of control system.

which have different characteristics each other. The state space expression of the actuator 1 is represented as follows;

$$P_1 \quad \begin{cases} \dot{x}_{11} = A_{11}x_{11} + B_{11}u_{11} \\ y_{11} = C_{11}x_{11}, \end{cases} \tag{1}$$

$$P_2 \quad \begin{cases} \dot{x}_{12} = A_{12}x_{12} + B_{12}u_{12} \\ y_{12} = C_{12}x_{12}. \end{cases} \tag{2}$$

If we assume that a force applied to actuator 1 is f_{l1}, then we have $u_{12} = y_{11} - f_{l1}$, so that,

$$\begin{bmatrix} \dot{x}_{11} \\ \dot{x}_{12} \end{bmatrix} = \begin{bmatrix} A_{11} & 0 \\ B_{12}C_{11} & A_{12} \end{bmatrix} \begin{bmatrix} x_{11} \\ x_{12} \end{bmatrix} + \begin{bmatrix} B_{11} \\ 0 \end{bmatrix} u_{11} + \begin{bmatrix} 0 \\ B_{12} \end{bmatrix} f_{l1}, \tag{3}$$

$$y_{12} = \begin{bmatrix} 0 & C_{12} \end{bmatrix} \begin{bmatrix} x_{11} \\ x_{12} \end{bmatrix}. \tag{4}$$

The augmented system can be written as

$$\dot{x}_1 = A_1x_1 + B_1u_1 + B_{l1}f_{l1} \tag{5}$$

$$y_1 = C_1x_1, \tag{6}$$

where, $x_1 = [x_{11}^T \; x_{12}^T]^T, y_1 = y_{12}$. As same as the actuator 1, the system of actuator 2 is represented as;

$$\dot{x}_2 = A_2x_2 + B_2u_2 + B_{l2}f_{l2} \tag{7}$$

$$y_2 = C_2x_2. \tag{8}$$

From (5) and (7), an augmented system of the total system is obtained as

$$\dot{x} = Ax + Bu + B_lf_l, \tag{9}$$

where,

$$x = \begin{bmatrix} x_1^T & x_2^T \end{bmatrix}^T, \quad f_l = \begin{bmatrix} f_{l1} & f_{l2} \end{bmatrix}^T,$$
$$A = \begin{bmatrix} A_1 & 0 \\ 0 & A_2 \end{bmatrix}, \quad B = \begin{bmatrix} B_1 & 0 \\ 0 & B_2 \end{bmatrix}, \quad B_l = \begin{bmatrix} B_{l1} & 0 \\ 0 & B_{l2} \end{bmatrix}.$$

We add a constraint condition that outputs of both actuators are equal, which means that the actuators attached to a common object. It is written by

$$y_1 = y_2, \tag{10}$$

that is,

$$C_1x_1 - C_2x_2 = 0. \tag{11}$$

The following equation is necessary to satisfy equation (11),

$$\begin{bmatrix} C_1 & -C_2 \end{bmatrix} \begin{bmatrix} \dot{x}_1 \\ \dot{x}_2 \end{bmatrix} = 0. \tag{12}$$

Since the constraint force is $\lambda = f_{l1} = -f_{l2}$, we have

$$\begin{bmatrix} E & B_l' \\ J & 0 \end{bmatrix} \begin{bmatrix} \dot{x} \\ \lambda \end{bmatrix} = \begin{bmatrix} Ax + Bu \\ 0 \end{bmatrix}. \tag{13}$$

Here, $x = [x_1^T \; x_2^T]^T$, $B_l' = [B_{l1}^T \; -B_{l2}^T]^T$, $J = [C_1 \; -C_2]$, and E is a unit matrix of an appropriate dimension. By deleting the constraint force λ in the equation, we obtain the following equations,

$$\dot{x} = A_cx + B_cu, \tag{14}$$

where,

$$M = \begin{bmatrix} E & B_l' \\ J & 0 \end{bmatrix}, \quad A_c = [E \mid 0] \; M^{-1} \begin{bmatrix} A \\ 0 \end{bmatrix},$$
$$B_c = [E \mid 0] \; M^{-1} \begin{bmatrix} B \\ 0 \end{bmatrix}.$$

B. Design of H_∞ controller

We design a feed-forward controller for the system (14) by applying H_∞ control theory. We show the block diagram of the system to be designed in Fig. 6. $M(s)$ is a target model, $C(s)$ is the H_∞ controller, and $P(s)$ is the system of the actuator. w is an external signal and z is an error between output y and the reference signal w. We design a controller $C(s)$ such that H_∞ norm of transfer function from w to z is minimized. We set $M(s)$ as a 3rd order Butterworth low-pass filter. Then, we use 'hinfsyn' function in MATLAB to design the controller.

C. Results

We evaluate the performance of the actuator with the H_∞ controller by a bode diagram. Figure 7 shows the gain plots of the target model and the controlled system. It shows that the controlled system is matched to the target model very well.

Next, in order to confirm the efficiency of coupling, the characteristics of the feed-forward controller will be compared with those of Na^+ or TEA^+ only.

Figure 8 is the frequency characteristics of the feed-forward controller for IPMC actuator using only Na^+ or TEA^+ and the H_∞ controller. In the figure, H_∞-Na^+ and H_∞-TEA^+ show

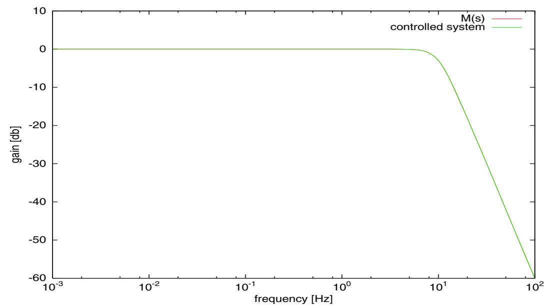

Fig. 7. Frequency property of the H_∞ controlled system.

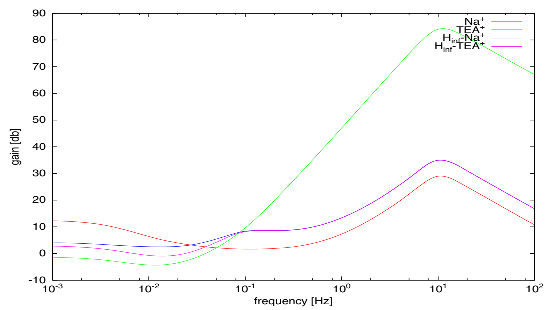

Fig. 8. Frequency property of the feed-forward controller.

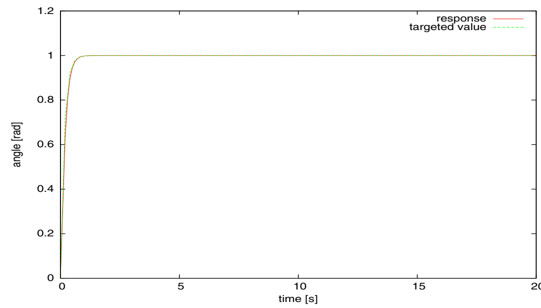

(a)

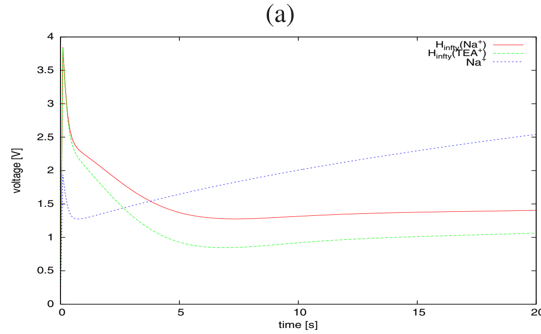

(b)

Fig. 9. Simulative results. (a) Output. (b) Input voltage.

the frequency gains of ω to u_1, and ω to u_2, respectively. It shows that the gain of the H_∞ controller is lower than Na^+ or TEA^+. Figure 9 shows the simulative results of controlled system, and it can be seen that output well tracks the reference signal. Figure 9(b) shows the input voltage of IPMC actuators in the case of using "Na^+ and TEA^+" or "only Na^+". The case of "only TEA^+" is omitted since the input is too large. It shows that the coupled actuators can be operated by a smaller input voltage than that of Na^+ though the transient voltages are almost same.

III. IPMC Sensor System

As mentioned previously, it is well known that IPMC films generate electromotive force by deformation. By utilizing the property, we develop an IPMC sensor system. Since the characteristics of output voltages are dynamic, we should compensate for the dynamics to estimate the deformation of IPMC sensor film. Then we identify the dynamics from input-output data as a linear time-invariant (LTI) system as before, and construct a sensor system using an observer based on the linear system control theory.

A. Identification of Sensor Dynamics

As well as the model of the IPMC actuator in the previous section, we identify the dynamics of the IPMC sensor from input-output data as a linear time invariant (LTI) system.

The IPMC films that we used in the experiment are Nafion® 117 (DuPont) plated with gold. The thickness of the thin films is about 200μm in a wet condition, and it was cut into a rectangular pieces of width 2mm and of length 20 mm.

Figure 10 shows a comparison between an experimental result and a simulative result of the identified model. It is observed that the characteristics of the IPMC sensor are captured enough. From this result, it seems that dynamics of the IPMC sensor can be modeled as a LTI system in this operating range.

As same as an IPMC actuator, the characteristics of IPMC sensor highly depend on the type of the counter ions. We also verify the doping effect of IPMC sensor. Figure 11 shows the gain property of IPMC sensors which are doped with sodium (Na^+) and tetraethylammonium (TEA^+) respectively. Each property is plotted using the identified model. From this figure, it can be seen that IPMC changes the sensing characteristics with respect to the doped counter ions. In this case, the sensor doped with TEA^+ is superior to that with Na^+ because of large gain and wide band.

B. Design of Sensor System Using Observer

In order to estimate the displacement or deformation from output voltage of IPMC sensor film, we apply an observer based on the linear system control theory.

The model of the sensor can be represented as

$$\begin{cases} \dot{x} = Ax + Bu \\ y = Cx + Du \end{cases} \tag{15}$$

where y is the output of the system whose output voltage, u is the input of the system which is displacement or deformation of IPMC sensor, and x is a state of the system.

Assuming that the variation of the input is not fast, that is,

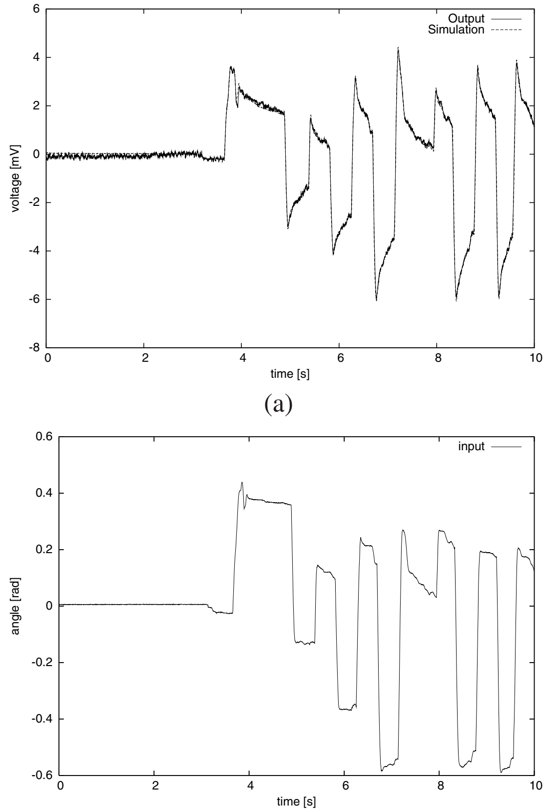

(a)

(b)

Fig. 10. Result of identification. (a) simulative results of output voltage. (b) Displacement.

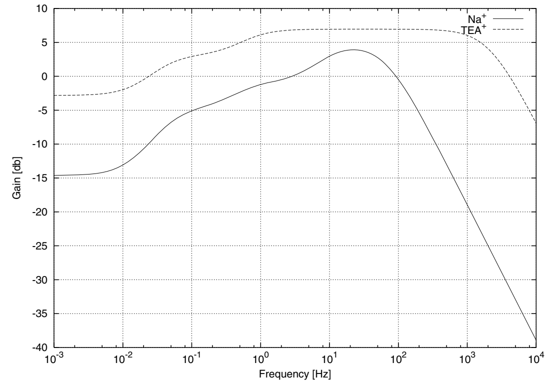

Fig. 11. Gain property of IPMC sensor.

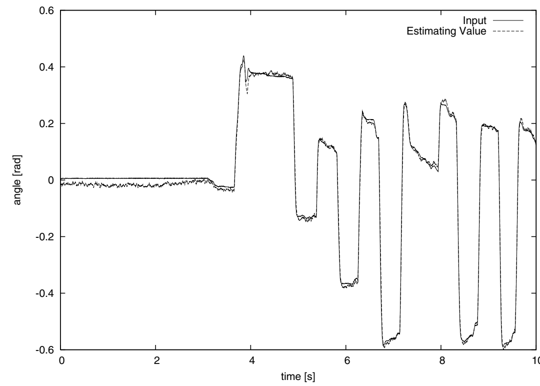

Fig. 12. results of estimations of IPMC sensor system. (Estimation of displacement.)

$\dot{u} \approx 0$, then the augmented system is represented as

$$\begin{cases} \dot{\bar{x}} = \bar{A}\bar{x} \\ y = \bar{C}\bar{x} \end{cases} \tag{16}$$

where, $\bar{x} = [x, u]^T$ is the state of the augmented system, and

$$\bar{A} = \begin{bmatrix} A & B \\ 0 & 0 \end{bmatrix}, \quad \bar{C} = \begin{bmatrix} C & D \end{bmatrix}.$$

If the system of Eq. (16) is observable, the input u can be estimated by an observer, since the input u is a part of the state of the augmented system.

In this paper, we construct the observer based on the stationary Kalman Filter. The observer is represented as

$$\dot{\hat{x}} = (\bar{A} - K\bar{C})\hat{x} + Ky \tag{17}$$

where, K is a gain matrix of optimal observer. The matrix K is leaded as

$$K = PC^T R^{-1}. \tag{18}$$

P is a positive definite symmetric matrix and a solution of Riccati equation which is described as follows:

$$PA^T + AP - PC^T R^{-1} CP + Q = 0 \tag{19}$$

where, Q, R are the covariance matrices of the assumed noise.

We constructed the sensor system based on the observer as the above procedure, and verify the performance of the sensor system. Figure 12 shows the experimental results on the estimation of the bending angle of the sensor film. By utilizing the identified model and observer, the bending angle of the sensor film can be measured with high accuracy.

C. Experiment of Feedback Control

In order to confirm the validity of the sensor system, we conducted an experiment of a position control using IPMC actuator/sensor. In the experiments, pair of IPMC films are connected in parallel. One of the IPMC films is used as an actuator, and another is used as a sensor. Then the bending angle of the IPMC actuator is controlled using the estimated value of bending angle from the sensor system. Experimental results are discussed in comparison with true value of the bending angle which is measured by a laser displacement sensor.

In this feedback experiment, we used the IPMC sensor doped with TEA^+ because of the characteristics of large gain and wide band as compared to that of Na^+ . On the other hand, we used the IPMC actuator doped with Na^+ because of the fast response. It is worth noted that different or complementally counter-ions are selected for the closed loop system to have a

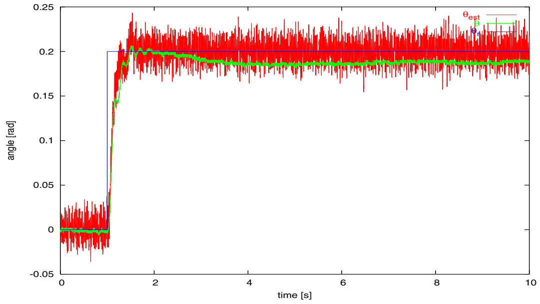

(a)

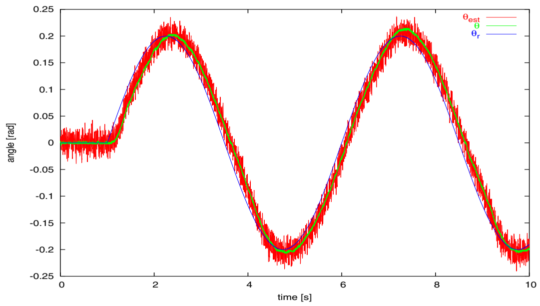

(b)

Fig. 13. Experimental results of feedback control. (a) Step response. (0.2 rad) (b) Sine wave response. ($0.2\sin(0.5t)$ rad)

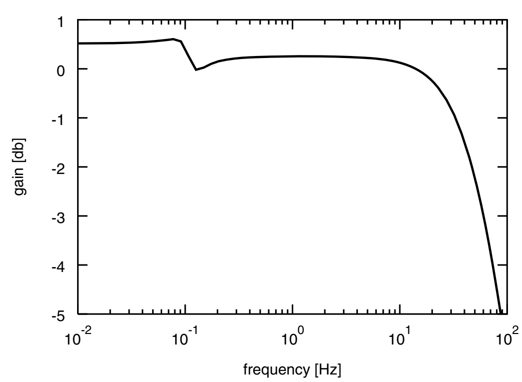

Fig. 14. Frequency characteristics of sensor system.

high loop gain.

Figure 13 shows the experimental results of position control using the signal of the IPMC sensor system. The figure plots the estimated, real, and reference angle over time. The IPMC is controlled in position by a PID controller. It can be seen that the estimation of position and feedback control were realized sufficiently though some errors of estimation are remained.

The stationary error of the estimation was appeared as a result of changes of dynamical characteristics, and it seems to be caused by changes of wet condition of IPMC films. The stationary error may be removed by keeping the condition, e.g. coating the films perfectly or using in the water.

Figure 14 shows the frequency characteristics of sensor system. It can be seen that wide bandwidth up to 50 Hz is realized.

IV. Conclusion

It can be considered that it is efficient to combine several IPMC actuators doped with various counter-ions, which have different characteristics. In this paper, we designed the feed-forward controller for the combined IPMC actuators based on H_∞ control theory, and evaluated its efficiency. In this paper, the designed controller is a feed-forward one, however, feedback controllers also can be designed easily in the same manner.

Also, we showed a method how to make a position sensor with IPMC film and demonstrated the sensor performance. We constructed a position feedback control system with the developed sensor system and it was shown that good responses can be obtained for a step or sinusoidal reference signals. Future researches may be more compact sensor/actuator integrated system design with IPMC films.

References

[1] K. Oguro et al., "Bending of an ion-conducting polymer film-electrode composite by an electric stimulus at low voltage," *Journal of Micromachine Society*, 5, 27-30, 1992. (in Japanese)

[2] Y. Bar-Cohen, *Electroactive polymer (EAP) actuators as artificial muscles: reality, potential, and challenges*, SPIE Press, 2001.

[3] M. Mojarrad and M. Shahinpoor, "Biomimetic robotic propulsion using polymeric artificial muscles," *Proc. of IEEE Int. Conf. on Robotics and Automation*, pp.2152-2157, 1997.

[4] S. Guo et al., "A New Type of Fish-Like Underwater Microrobot," *IEEE/ASME Trans. on Mechatronics*, Vol. 8, No. 1, pp.136-141, 2003.

[5] EAMEX Corporation, http://www.eamex.co.jp/

[6] J. Jung et al., "Undulatory tadpole robot (TadRob) using ionic polymer metal composite (IPMC) actuator," *Proc. of IEEE/RSJ Int. Conf. on Intelligent Robots and Systems*, pp.2133-2138, 2003.

[7] Y. Nakabo et al., "Biomimetic soft robot using artificial muscle," *in tutorial "Electro-Active Polymer for Use in Robotics", IEEE/RSJ Int. Conf. on Intelligent Robots and Systems*, 2004.

[8] Y. Bar-Cohen et al., "Challenges to the application of IPMC as actuators of planetary mechanisms," *Proc. of SPIE Int. Symp. on Smart Structures and Materials, EAPAD*, Vol. 3987, 2000.

[9] S. Tadokoro et al., "Modeling IPMC for design of actuation mechanisms," *Electroactive Polymer (EAP) Actuators as Artificial Muscles, Reality, Potential, and Challenges*, Ed. Y. Bar-Cohen, SPIE Press, pp.331-366, 2001.

[10] K. Onishi et al., "The effects of counter ions on characterization and performance of a solid polymer electrolyte actuator," *Electrochemica Acta*, Vol. 46, No. 8, pp.1233-1241, 2001.

[11] M. Mojarrad and M. Shahinpoor, "Ion-Exchange-Metal Composite Sensor Films," *Proc. of SPIE, Smart Structures and Materials, Smart Sensing, Processing, and Instrumentation*, Vol. 3042, pp.52-60, 1997.

[12] M. Shahinpoor, Y. Bar-Cohen, J. O. Simpson and J. Smith, "Ionic Polymer Metal Composites (IPMCs) as Biomimetic Sensors, Actuators and Artificial Muscles - A Review," *Smart Materials and Structures*, Vol. 7, No. 6. 1998.

[13] M. Konyo et al., "Development of Velocity Sensor Using Ionic Polymer-Metal Composites," *Proc. of SPIE Int. Symp. on Smart Structures and Materials, EAPAD*, Vol. 5385, pp.307-318, 2004.

[14] K. Mallavarapu et al., "Feedback control of the bending response of ionic polymer-metal composite actuators," *Proc. of SPIE Int. Symp. on Smart Structures and Materials, EAPAD*, Vol. 4329, pp.301-310, 2001.

[15] K. Asaka and K. Oguro, "Bending of polyelectrolyte membrane platinum composites by electric stimuli Part II. Response kinetics," *Journal of Electroanalytical Chemistry*, 480, pp.186-198, 2000.

[16] S. Tadokoro et al., "A dynamical model of ICPF actuator considering ion-induced lateral strain for molluskan robotics," *Proc. of IEEE Int. Conf. on Robotics and Automation*, pp. 2010-2017, 2002.